Int. Conf. on Jets, Wakes and Separated Flows, ICJWSF-2017
October 9-12, 2017, Cincinnati, Ohio USA

A LES STUDY ON THE EFFECT OF PERIODIC GUSTS ON A TRUCK MODEL

*[1]G. Minelli, *[2]B. Basara and *[1]S. Krajnović

[1]Department of Mechanics and Maritime Sciences,
Chalmers University of Technology, Gothenburg 41296, Sweden.
minelli@chalmers.se

[2]AVL List GmbH, Advanced Simulation Technologies, Graz, Austria.

ABSTRACT

This work presents an application of the Large Eddy Simulation Coherent Structures Model (LES-CSM) equations for an external vehicle flow. In particular, the flow around a generic truck is simulated. The model is forced to oscillate in order to represents a more realistic ground vehicle flow condition, where gusts (of different natures) define the unsteadiness of the incoming flow. In this numerical study, the Reynolds number is $Re = 4 \times 10^4$ based on the width of the model $W = 0.152$ and the incoming velocity $U_{inf} = 4.26$m/s. The model is forced to oscillate with a yaw angle $10° > \beta > -10°$ and a non-dimensional frequency $St = fW/U_{inf} = 0.06$. The effect of the periodic motion of the model is compared with the quasi-static flow condition. Overall, the effect of oscillation changes drastically the flow, arising an hysteresis behaviour and complete different features, when compared to the static configuration. This study is relevant to better understand real flow conditions, with the ultimate goal to implement an effective active flow control strategy for aerodynamic drag reduction.

1 INTRODUCTION

Both numerical and experimental quasi-static studies represent an idealized condition of the flow that surrounds cars and trucks during daily operations. The real flow is indeed fundamentally different from the controlled and clean flow reproduced in a wind tunnel test section or simulated by CFD platforms. For example, the stability of a travelling truck is affected by wind gusts from its front and sides. As a consequence, the aerodynamic effect creates a dynamic force that causes the driver to overreact, which further increases the dynamic instability of the vehicle. Typical examples of these sudden gusts can be experienced in different scenarios: when entering or exiting areas sheltered from the wind such as tunnels or passing buildings, by strong wind gusts, by the passing of two vehicles or atmospheric turbulence. For this reason, after a first quasi-static approach, used to develop the main aerodynamic features of a road vehicle, it is of main importance to verify the flow behaviour under real conditions. The straight forward solution is to perform "on road" experiments, which verify directly the aerodynamic performance of a model or a prototype. On the other hand, this approach does not allow to understand the flow features, a crucial step to develop better and effective aerodynamic solutions. For this reason, would be fruitful to recreate a real "on road" condition to be studied in a controlled environment like a wind tunnel test section or using CFD. With this in mind, the use of an oscillating model to recreate realistic flow conditions was first explored in [1] and later investigated numerically and experimentally for a simplified car model in [2] and [3], respectively. More recently, using a CFD approach, an active flow control solution has also been optimized under a gusty flow condition [4]. All these works confirm that the flow nature changes significantly from the quasi-static to the dynamic configuration, stressing the importance of pursuing more realistic tests during the design process of aerodynamic devices. Two main parameters are chosen to parametrize the oscillation of the model. The first one is the oscillation frequency, chosen for this study as $St = fW/U_{inf} = 0.06$, and the second one is the yaw angle range $10° > \beta > -10°$. These choices are supported by the aforementioned "on road" experiments [5, 6, 7], which highlight the range of important frequencies in cross wind studies between $0.06 > St > 0.9$ and a most common lateral wind speed of about 4-5 m/s [5] which, in particular, leads to the choice of the yaw angle range. In this study a two-bodied truck model

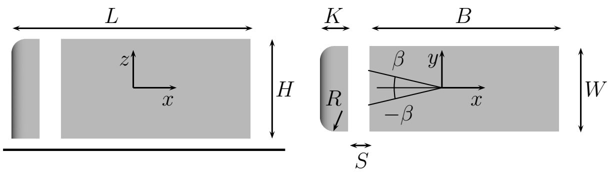

Figure 1: The model.

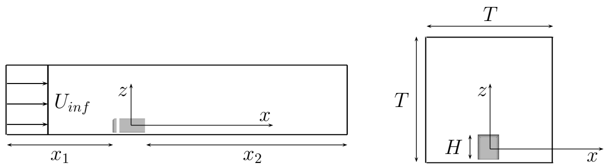

Figure 2: The computational domain.

with rounded corners at the top front of the cabin (same model as in [1]), is oscillating with a yaw angle β. The Reynolds number, based on the inlet velocity of 4.26 m/s and the width of the model W, is $Re = 4 \times 10^4$. This work is a step toward the implementation of an active flow control for a real truck configuration, and it develops from the previous achievements in flow structures analysis and flow control collected in [8, 9]. In particular at this stage we want to pursue the following goals:

- Run a dynamic, unsteady LES simulation at a relatively high Reynolds number of a simplified truck model.
- Investigate the discrepancy between quasi-static and dynamic flow conditions.
- Point out the main flow behaviour for a future implementation of aerodynamic solutions like active flow control.

2 NUMERICAL SET-UP

LES-CSM were employed for the numerical study of the flow around an oscillating truck model. The following boundary conditions were applied to all simulations. A homogeneous Neumann boundary condition was applied at the outlet. The surfaces of the body were treated as no-slip walls, while the wind tunnel walls were defined as symmetry walls.

Table 1: Dimension of the model. All dimensions are scaled by the model width $W = 0.152$ m.

W	H	K	B	S	R
1	1.164	0.342	2.217	0.25	0.166

Table 2: Dimension of the computational domain. All dimensions are scaled by the model width $W = 0.152$ m.

x_1	x_2	T
9.368	17.5	6

Table 3: Details of the computational grid.

# of cell	y^+_{mean}	Δs^+_{max}	Δl^+_{max}
11 millions	< 0.6	< 60	< 35

The oscillation of the model around the vertical axis (z) was obtained by deforming the computational grid. The deformation of the grid was made only in a circular region around the model. The simulations in this work are made with the commercial finite volume CFD solver, AVL FIRE [10]. AVL FIRE is based on the cell-centred finite volume approach. Concerning the mesh resolution, a reliable LES grid should resolve 80% of the turbulent energy [11]. In order to achieve this and resolve the near wall turbulent structures of the flow, the first grid point in the wall normal direction must be located at $n^+ < 1$, where $n^+ = \frac{u_\tau n}{\nu}$ with the friction velocity u_τ, while the resolutions in the span-wise and stream-wise directions must be $\Delta l^+ \simeq 15 - 40$ and $\Delta s^+ \simeq 50 - 150$ respectively [12]. Here, $\Delta l^+ = \frac{u_\tau \Delta l}{\nu}$ and $\Delta s^+ = \frac{u_\tau \Delta s}{\nu}$. In this work, the grid resolution has an average value in the wall normal direction of $n^+ = 0.6$ and a maximum value of $n^+ = 3$ only at the front edges of the cabin, where the acceleration of the flow is maximum. The resolutions in the span-wise and stream-wise directions are reported in Tab. 3. The chosen time step, $\Delta t^* = \Delta t U_{inf}/W$, is $\Delta t^* = 2.8 \times 10^{-3}$ for all simulations, resulting in a CFL number lower than 1 in the entire domain. All simulations were run first until the flow was fully developed. This was followed by an averaging of $t^* = tU_{inf}/W = 90$ that corresponds to three flow passages through the computational domain.

The LES-CSM equations

The governing LES equations are the spatially implicitly filtered Navier-Stokes equations, where the spatial filter is determined by the characteristic width $\Delta = (\Delta_1 \Delta_2 \Delta_3)^{\frac{1}{3}}$, and Δ_i is the computational cell size in the three coordinate directions.

$$\frac{\partial \bar{u}_i}{\partial t} + \frac{\partial}{\partial x_j}\left(\bar{u}_i \bar{u}_j\right) = -\frac{1}{\rho}\frac{\partial \bar{p}}{\partial x_i} + \nu \frac{\partial^2 \bar{u}_i}{\partial x_j \partial x_j} - \frac{\partial \tau_{ij}}{\partial x_j} \quad (1)$$

and

$$\frac{\partial \bar{u}_i}{\partial x_i} = 0. \tag{2}$$

Here, $\bar{u}_i$ and $\bar{p}_i$ are the resolved velocity and pressure, respectively, and the bar over the variable denotes the operation of filtering. The influence of the small scales in Eq. 1 appears in the SGS stress tensor, $\tau_{ij} = \overline{u_i u_j} - \bar{u}_i \bar{u}_j$. The coherent-structure Smagorinsky model (CSM) proposed by Kobayashi [13] is used in this work. The Smagorinsky model represents the anisotropic part of the SGS stress tensor, τ_{ij} as

$$\tau_{ij} - \frac{1}{3}\delta_{ij}\tau_{kk} = -2\nu_{sgs}\bar{S}_{ij} \tag{3}$$

where the SGS viscosity,

$$\nu_{sgs} = (C\Delta)^2 |\bar{S}| \tag{4}$$

and,

$$|\bar{S}| = \sqrt{(2\bar{S}_{ij}\bar{S}_{ij})} \tag{5}$$

where

$$\bar{S}_{ij} = \frac{1}{2}\left(\frac{\partial \bar{u}_i}{\partial x_j} + \frac{\partial \bar{u}_j}{\partial x_i}\right). \tag{6}$$

The model parameter, C, in the CSM is determined as follows

$$C = C_1 |F_{CS}|^{3/2} F_{\Omega} \tag{7}$$

where $C_1 = 1/22$ is a model constant, $F_{CS} = Q/E$ is the coherent-structure function (CSF) and $F_{\Omega} = 1 - F_{CS}$ is the energy decay suppression function. Q is the second invariant of the velocity gradient tensor

$$Q = -\frac{1}{2}\left(\frac{\partial \bar{u}_i}{\partial x_j}\frac{\partial \bar{u}_j}{\partial x_i}\right) \tag{8}$$

and E is the magnitude of the velocity gradient tensor

$$E = \frac{1}{2}\left(\frac{\partial \bar{u}_j}{\partial x_i}\right)^2. \tag{9}$$

3 RESULTS

A static study of three different yawed configurations, between 0 and 10 degrees, is reported and compared with the dynamic study of the flow. Figure 3 shows the force history during one complete averaged yaw sweep when compared to the static configuration forces, while Figs. 4 to 7 show the difference in the flow structures between the static and the dynamic configurations at the same yaw angle. The fluctuations, introduced by the periodic movement of the model, drastically change the aerodynamic performance. Figure 4 shows that the periodic oscillation of the model, even within a limited yaw angle, brings to a complete separated flow region on one side of the truck, depending on the oscillation sign. This affects significantly the stability of the vehicle, and the driver might experience a lateral force even if the apparent yaw angle is $\beta = 0°$. Figures 4 and 5 are representative of the hysteresis effect visible in Fig. 3(b). In particular, at the same yaw angle $\beta = 5°$, the vehicle experiences a strong lateral force according to the direction of the wind gust. Taking a closer look to the flow structures on the top of the trailer, Fig. 6, one can observe the roll up of a clear and long stream-wise vortex due to the influence of the inertial force generated by the model rotation. This vortex also contributes to a drag increase visible in Fig. 3(a) (solid line from 10° to 0° at $\beta = 5°$) when compared to the static configuration (dot at $\beta = 5°$). It is interesting to observe the flow behaviour at $\beta = 10°$, Fig. 7. In particular, the static solution gives 40% higher drag value when compared to the dynamic simulation value at $\beta = 10°$). In fact, for the oscillating case, the side separated flow does not directly interact with the wake and tends to reattach on the trailer of the model, Fig.7 (c). Figure 8 shows a complete sweep from $\beta = 0°$, where the counter clock rotation (Fig. 8(a-e)) is followed by the consequent clock wise rotation (Fig. 8(f-h)). The inertial effect, of the rotation sign change, is clearly visible. The wake is never aligned to the model, as it was for the static case, and the flow at the leeward side is almost attached to the lateral surface of the model while the flow is fully separated on the windward side when we consider counter clock wise rotations (Fig. 8(a-e)). On the other hand, in Fig. 8(f) the sign change has just occurred and the inertia of the flow create a separated region switch from the windward to the leeward side.

Observing this comparison, it is clear that a gusty flow condition (formed by the oscillation of the model) produces a fundamentally different flow from the quasi-static configuration. Thus, it is of main importance to investigate further and understand the possibilities of an active flow control under these conditions.

4 CONCLUSIONS

The case studied here consists of the numerical investigation of a double-bodied truck model. Static and dynamic LES are performed and compared to study the effect of gusts when compared to standard static flow condition. To reproduce a gusty flow state, the model is forced to oscillate between

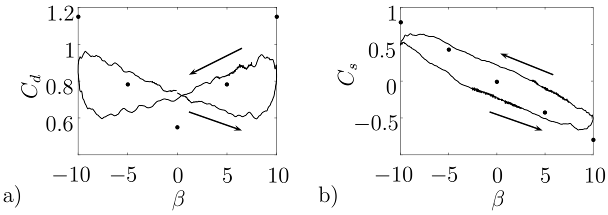

Figure 3: C_d (a) and C_s (b). Comparison between the static (dots) and the dynamic (solid line) case.

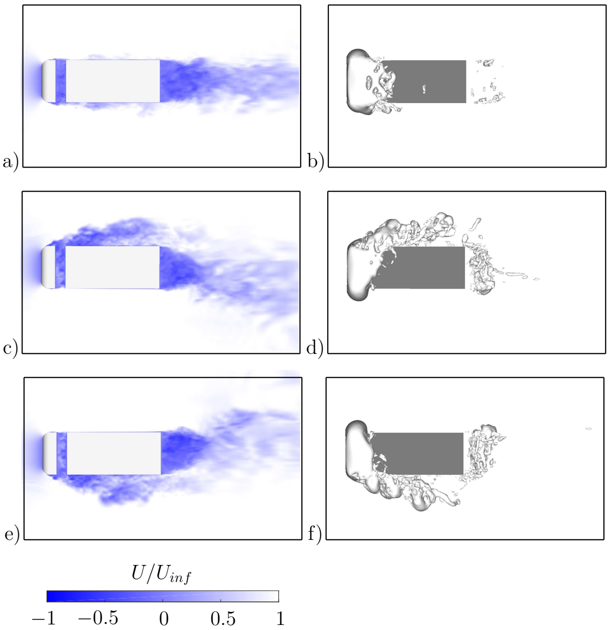

Figure 4: The static (a and b), the dynamic configuration at $\beta = 0°$ during a counter clock wise (positive) rotation (c and d) and a clock wise (negative) rotation (e and f). Instantaneous streamwise flow velocity (a, c and e) and isosurfaces of the instantaneous pressure field (b, d and f).

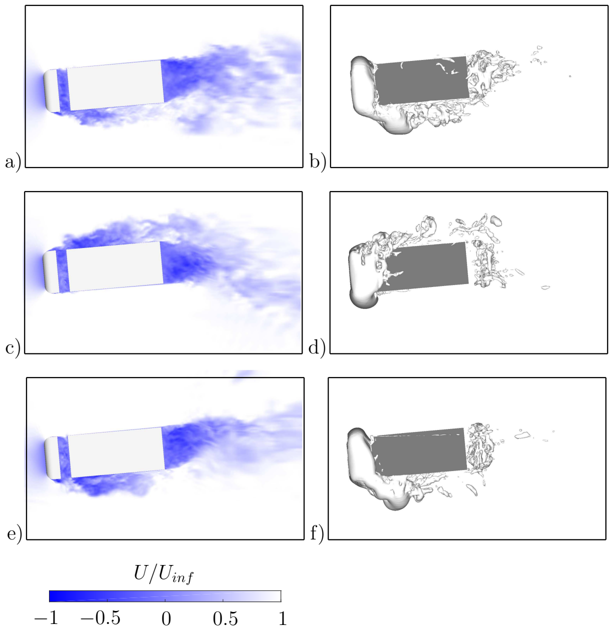

Figure 5: The static (a and b), the dynamic configuration at $\beta = 5°$ during a counter clock wise (positive) rotation (c and d) and a clock wise (negative) rotation (e and f). Instantaneous streamwise flow velocity (a, c and e) and isosurfaces of the instantaneous pressure field (b, d and f).

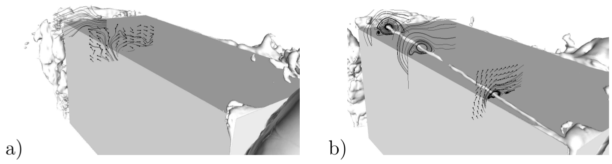

Figure 6: A particular of the flow over the trailer. Static (a) at $\beta = 5°$ and dynamic (b) at $\beta = 5°$ during a clock wise rotation.

a yaw angle $-10° < \beta < 10°$, achieved by deforming the mesh around the truck. By doing this, the model experiences gusts that typically characterize the daily "on-road" operations of a generic transport vehicle. As mentioned earlier, with this study we want to gain a better knowledge of the flow features of a realistic condition. This is important when it comes down to aero design and development of aerodynamic solutions like an active flow control. In closing, in this work we want to highlight the following points:

- LES-CSM can be used as a preliminary tool to investigate such a flow condition.
- The flow feature of a dynamic oscillating configuration drastically change the aerodynamic performance, even if the yaw angle considered is relatively small.
- Gusts modify the apparent angle of the flow impinging the vehicle, giving inertia and momentum to the flow.
- An active flow control should be design in a way to taking into account these conditions, and it should adjust considering the conditions of the incoming flow.

ACKNOWLEDGEMENTS

Software licenses were provided by AVL List GMBH. Computations were performed at SNIC (the Swedish National Infrastructure for Computing) at the National Supercomputer Center (NSC)

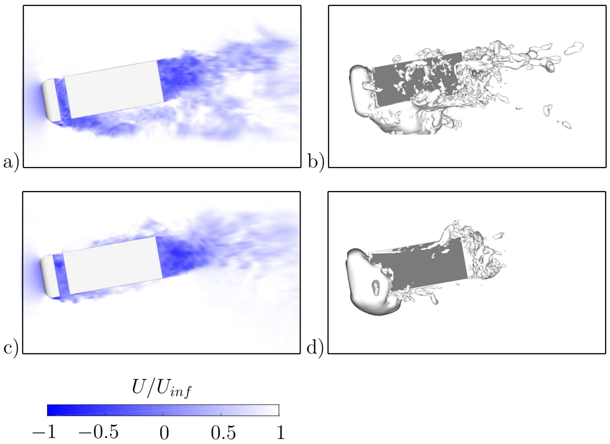

Figure 7: The static (a and b) and the dynamic (c and d) configuration at $\beta = 10°$. Instantaneous stream-wise flow velocity (a and c) and isosurfaces of the instantaneous pressure field (b and d).

at LiU.

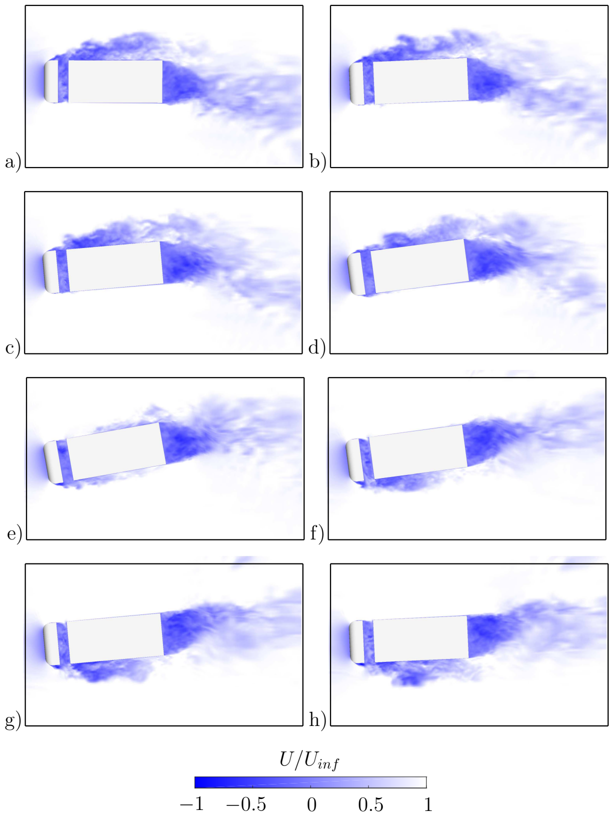

Figure 8: Instantaneous stream-wise flow velocity sequence. Positive rotation (a-e) and negative (f-h). $\beta = 0°$ (a), $\beta = 2.5°$ (b and h), $\beta = 5°$ (c and g), $\beta = 7.5°$ (d and f), $\beta = 10°$ (e).

REFERENCES

[1] Kevin P. Garry and Kevin R. Cooper. Comparison of quasi-static and dynamic wind tunnel measurements on simplified tractor-trailer models. *Journal of Wind Engineering and Industrial Aerodynamics*, 22(2-3):185–194, 1986.

[2] Sinisa Krajnovic, Anders Bengtsson, and Branislav Basara. Large Eddy Simulation Investigation of the Hysteresis Effects in the Flow Around an Oscillating Ground Vehicle. *Journal of Fluids Engineering*, 133(12):121103, 2011.

[3] Emmanuel Guilmineau and Francis Chometon. Numerical and Experimental Analysis of Unsteady Separated Flow behind an Oscillating Car Model. *SAE International Journal of Passenger Cars - Mechanical Systems*, 1(1):646–657, 2008.

[4] G Minelli, S Krajnović, and B Basara. PANS Study of the Flow Around an Oscillating, Simplified Truck Cabin with Flow Control. In *ASME 2017 Fluids Engineering Division Summer Meeting, FEDSM2017, Waikoloa, USA*, 2017.

[5] Simon Watkins and Jeffrey W Saunders. Turbulence Experienced by Road Vehicles under Normal Driving Conditions. *SAE Technical Paper Series*, 1995.

[6] Scott Wordley and Jeff Saunders. On-road Turbulence. 2008.

[7] Scott Wordley and Jeff Saunders. On-road Turbulence: Part 2. 2(1):111–137, 2009.

[8] G Minelli, S Krajnović, B Basara, and B R Noack. Numerical Investigation of Active Flow Control Around a Generic Truck A-Pillar. *Flow, Turbulence and Combustion*, 97(4):1235–1254, 2016.

[9] G Minelli, E Adi Hartono, V Chernoray, L Hjelm, S Krajnović, and B Basara. Validation of pans and active flow control for a generic truck cabin. *Journal of Fluid Mechanics*, Under review.

[10] AVL. Fire manual v2014. 2014.

[11] Stephen B Pope. *Turbulent Flows*. 2001.

[12] Ugo Piomelli and J.R. Chasnov. *Large-eddy simulations: theory and applications*. Kluwer Academic Publisher, 1996.

[13] Hiromichi Kobayashi. The subgrid-scale models based on coherent structures for rotating homogeneous turbulence and turbulent channel flow. *Physics of Fluids*, 17(4), 2005.